Electron transmission across an interface of different one-dimensional crystals

Anatoly A. Grinberg and Serge Luryi
AT&T Bell Laboratories, Murray Hill, New Jersey 07974
(Received 17 October 1988)

An exact solution is obtained for the quantum-mechanical reflection and transmission coefficients for the electronic motion across the boundary of two different one-dimensional crystals, each described by a Kronig-Penney model. The result is compared with those obtained in the envelope-function (plane-wave) approximations with different degrees of refinement. It turns out that, in general, *neither* the simplest such approximation, corresponding to a continuous envelope function Φ and a discontinuous gradient Φ' (with a single-parameter matching of the electron flux $m^{-1}\Phi'$ across the interface), *nor* the refined procedure, originally proposed by Harrison (corresponding to a two-parameter matching of discontinuous Φ and Φ' subject to the flux-continuity condition), produce an adequate description. Only with a special assumption about the size of the crystal cell at the interface do these procedures provide a consistent approximation; for this case we have derived an explicit expression for the matching coefficients in terms of "crystal" structure parameters. For arbitrary sizes of the boundary cell, the exact solution for the reflection coefficient in the vicinity of the band edges can be modeled with a three-parameter envelope-function approximation.

I. INTRODUCTION

The problem of electron transmission through a boundary of two different crystals[1] often arises in heterojunction electronics as well as in transport properties of polycrystalline materials. Rigorous solution of such problems is intractable without extensive numerical work, since one must know both the exact Bloch functions in constituent materials and the evanescent states near the interface.[2-10] The common approach, therefore, has been to replace the Bloch functions by envelope functions (plane waves) and use the effective-mass approximation. Of course, the envelope function Φ and its derivatives need not be continuous across the interface, and the appropriate matching conditions are not known either. In principle, these conditions would follow from a valid expression for the current operator in terms of the envelope functions. Such an expression, if it exists, in turn depends on the proper form of the effective kinetic energy operator acting on the envelope functions and valid in regions where the band structure is rapidly varying (or, in the limit, abruptly changing across an interface). Although a number of self-consistent choices for this operator have been discussed in the literature,[1,11-14] it has never been generally derived from the first principles. Instructive results, however, have been obtained[15-19] in theories based on the Kane $\mathbf{k}\cdot\mathbf{p}$ model and the tight-binding approximation.

Following Harrison,[1] a number of authors have used the matching condition of continuous electron flux, expressed by the continuity of $\zeta\Phi$ and $(m\zeta)^{-1}\nabla\Phi$, where $m(x)$ is the effective electron mass and $\zeta(x)$ is a scalar parameter—hopefully not too strongly dependent on the energy near the band edge in each crystal. For one-dimensional crystals, Harrison's conditions in their most general form,[1]

$$\beta\Phi \text{ continuous}, \quad \alpha(\partial\Phi/\partial x) \text{ continuous}$$

can be justified by the fact that the effective Schrödinger equations, defining the envelope functions in each crystal, are second-order differential equations, and therefore their solutions can be matched with two parameters, α and β. However, one relation between these parameters follows from the conservation of flux. For example, if one assumes the following form of the current density:[1]

$$J_x = -\frac{\hbar}{2im_0}\left[\Phi^*\frac{\alpha\partial(\beta\Phi)}{\partial x} - \Phi\frac{\alpha\partial(\beta\Phi^*)}{\partial x}\right],$$

and if the effective-mass approximation is used for the electron energy spectrum, then the current continuity requires that $\alpha\beta m$ be continuous across the interface. The matching problem thus reduces to *one* unknown parameter (besides the effective mass m, regarded as known; of course, the flux continuity requirement will reduce the dimensionality of the parameter set to 1 with any assumption for the current density). It should be emphasized therefore, that one cannot expect, in general, that such a parameterization scheme will reproduce correct results (with any value of the remaining parameter, e.g., the above ζ)—unless the form of the current density is rigorously justified (derived from first principles). Nevertheless, this scheme is widely used and in many publications, especially those dealing with semiconductor device structures, ζ is simply set equal unity.[20,21] Although this approach is not rigorously justified, it has the advantage that the boundary conditions are defined in terms of the only known quantity m.

The purpose of the present work is to investigate the validity of such approximations by comparing them with an exact solution derived for the model problem of electron transmission across the boundary of two one-

dimensional crystals. These crystals are considered in the Kronig-Penney model[22] as periodic arrays of δ-function potential peaks. Both the strength of these peaks and the periodicity can be made different in the two crystals and in addition one can have a potential discontinuity at an interface plane. This permits us to isolate the band-structure effects from those associated with a potential step at the interface. The exact model and the envelope-function approximations will be compared with respect to the results they yield for the reflection and the transmission of electron waves incident on the interface.

II. ELECTRONIC WAVE FUNCTIONS IN TWO KRONIG-PENNEY CRYSTALS

This section serves mainly to introduce the model under consideration. The model is illustrated in Fig. 1. The left "crystal" is labeled 1, the right 2. The crystals represent arrays of δ functions of strength P_i and periodicity d_i, $i=1,2$. An important characteristic of the boundary is the size $b \equiv b_1+b_2$ of the cell containing "atoms" of both crystals. This is a source of uncertainty even in our model problem, because the reflection coefficient will be a strong function of b. In real crystals the situation is still more complicated because in the vicinity of the boundary the pseudopotential is distorted. We shall not restrict ourselves to any specific value of b, except in examples; for simplicity of presentation we shall assume that the gap between the two crystals is not too large: $b < d_1+d_2$. Then we can always choose the crystal unit cells so that they abut at $x=0$ without a gap or overlap. The Schrödinger equation in these abutting cells is of the form

$$\frac{d^2\Psi_{k_i}^{(i)}}{dx^2}+\left[q_i^2+\frac{2m_0P_i}{\hbar^2}\delta(x\pm b_i)\right]\Psi_{k_i}^{(i)}=0, \quad i=1,2 \tag{1}$$

where

$$\hbar q_1=\sqrt{2m_0E} \text{ and } \hbar q_2=\sqrt{2m_0(E-V)} ,$$

m_0 is the free-electron mass, E the electron energy, and V a potential barrier at the interface. The (+) sign in the δ-function argument is used when $i=1$ and (−) when $i=2$.

The Bloch solutions of Eq. (1) satisfy the relation

$$\begin{aligned}\Psi_{k_1}^{(1)}(0)&=e^{ik_1d_1}\Psi_{k_1}^{(1)}(-d_1) ,\\ \Psi_{k_2}^{(2)}(d_2)&=e^{ik_2d_2}\Psi_{k_2}^{(2)}(0) .\end{aligned} \tag{2}$$

From Eq. (2) and a similar relation for the wave-function derivative one obtains the well-known Kronig-Penney dispersion equations

$$\cos(k_id_i)=\cos(q_id_i)-U_i\frac{\sin(q_id_i)}{q_id_i}, \quad i=1,2 \tag{3}$$

where

$$U_i\equiv\frac{m_0P_id_i}{\hbar^2} , \tag{4}$$

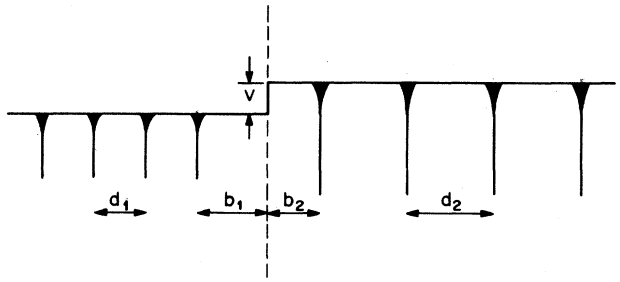

FIG. 1. Illustration of the model. Two crystals, adjacent at $x=0$, are formed by periodic arrays of δ-function potentials of the form $-P_i\delta[x\pm(b_i+nd_i)]$, $n=0,1,2,\ldots$, where the (+) sign refers to the left crystals ($i=1$) and the (−) sign to the right crystal ($i=2$).

and the wave functions are of the form

$$\Psi_{k_i}^{(i)}(x)=A_{k_i}\left[\frac{1-e^{-i(q_i+k_i)d_i}}{1-e^{-i(q_i-k_i)d_i}}e^{iq_i(x\pm b_i)}+e^{-iq_i(x+b_i)}-(1-e^{-i(q_i+k_i)d_i})e^{iq_i|x\pm b_i|}\right] , \tag{5}$$

where the (+) sign corresponds to $i=1$ and (−) to $i=2$, and A_{k_i} are normalization constants. Normalizing the wave functions to unity over one unit cell, we obtain

$$\left|\frac{A_{k_1}}{A_{-k_1}}\right|^2=\frac{\sin^2[(q_1-k_1)d_1/2]}{\sin^2[(q_1+k_1)d_1/2]} . \tag{6}$$

Besides the Bloch solutions (5), there exist evanescent-wave solutions of Eq. (1), exponentially localized near the interface.[23] These states, corresponding to electron energies in the bands forbidden by (3), do not affect the electron motion in the allowed bands. The fact that evanescent states can be ignored in our treatment of electron transmission across an interface of two crystals is a special feature of the one-dimensional case. In three (already in two) dimensions, the evanescent solutions mix with the Bloch functions at a given energy and play an essential role in the transmission process;[4,10,17] without them it would be impossible to match the solutions across a continuous boundary (line or surface).

III. DETERMINATION OF THE REFLECTION COEFFICIENT

The eigenfunctions $\Psi_{k_1}^{(1)}$ and $\Psi_{k_2}^{(2)}$ correspond to the electron motion with group velocities v_{k_1} and v_{k_2} in the left and the right crystals, respectively. In each crystal these functions are normalized to $\delta(k_i-k_i')$. Considering the reflection of a band electron incident on the interface from the left, the total wave function can be written in the form

$$\Psi(x)=\begin{cases}\Psi_{k_1}^{(1)}+r\Psi_{-k_1}^{(1)}, & x\le 0\\ t\Psi_{k_2}^{(2)}, & x\ge 0\end{cases} \tag{7}$$

where r and t are the reflection and the transmission amplitudes, respectively; these can be determined by matching the wave functions and their derivatives at the interface

$$\begin{aligned}&\Psi^{(1)}_{k_1}(0)+r\Psi^{(1)}_{-k_1}(0)=t\Psi^{(2)}_{k_2}(0)\ ,\\&\Psi^{(1)\prime}_{k_1}(0)+r\Psi^{(1)\prime}_{-k_1}(0)=t\Psi^{(2)\prime}_{k_2}(0)\ .\end{aligned}\tag{8}$$

From Eqs. (8) it follows that

$$r=\frac{\Psi^{(1)}_{k_1}(0)\Psi^{(2)\prime}_{k_2}(0)-\Psi^{(1)\prime}_{k_1}(0)\Psi^{(2)}_{k_2}(0)}{\Psi^{(1)\prime}_{-k_1}(0)\Psi^{(2)}_{k_2}(0)-\Psi^{(1)}_{-k_1}(0)\Psi^{(2)\prime}_{k_2}(0)}\ ,\tag{9}$$

$$t=\frac{\Psi^{(1)}_{k_1}(0)\Psi^{(1)\prime}_{-k_1}(0)-\Psi^{(1)\prime}_{k_1}(0)\Psi^{(1)}_{-k_1}(0)}{\Psi^{(1)\prime}_{-k_1}(0)\Psi^{(2)}_{k_2}(0)-\Psi^{(1)}_{-k_1}(0)\Psi^{(2)\prime}_{k_2}(0)}\ .\tag{10}$$

Substituting (5) into (9) we find the reflection amplitude in the form

$$r=\frac{(q_1+q_2)(\beta^{(1)*}_{(+)}\beta^{(2)*}_{(-)}e^{i\delta_{(+)}}-\beta^{(1)}_{(-)}\beta^{(2)}_{(+)}e^{-i\delta_{(+)}})-(q_1-q_2)(\beta^{(1)*}_{(+)}\beta^{(2)}_{(+)}e^{i\delta_{(-)}}-\beta^{(1)}_{(-)}\beta^{(2)*}_{(-)}e^{-i\delta_{(-)}})}{(q_1+q_2)(\beta^{(1)*}_{(-)}\beta^{(2)*}_{(-)}e^{i\delta_{(+)}}-\beta^{(1)}_{(+)}\beta^{(2)}_{(+)}e^{-i\delta_{(+)}})-(q_1-q_2)(\beta^{(1)*}_{(-)}\beta^{(2)}_{(+)}e^{i\delta_{(-)}}-\beta^{(1)}_{(+)}\beta^{(2)*}_{(-)}e^{-i\delta_{(-)}})}\ ,\tag{11}$$

where

$$\begin{aligned}&\beta^{(i)}_{(\pm)}\equiv 1-\exp(2i\alpha^{(i)}_{(\pm)}),\quad i=1,2\\&2\alpha^{(i)}_{(\pm)}\equiv(q_i\pm k_i)d_i,\quad \delta_{\pm}\equiv q_1b_1\pm q_2b_2\ .\end{aligned}\tag{12}$$

Inasmuch as the group velocities of incident and reflected electrons are equal, the intensity reflection coefficient is simply given by

$$R=|r|^2\ .\tag{13}$$

Let us consider in more detail the case of a zero potential barrier at the interface $V=0$ (and hence $q_1=q_2\equiv q$). This situation is rarely occurring in heterostructure transmission problems, but it will allow us to discuss the questions of principle regarding the effective-mass and the envelope-function approximations, without introducing additional complications peripheral to these questions. For $V=0$ we obtain from Eq. (11) the following expression for the transmission coefficient $T\equiv 1-R$:

$$T=\frac{[\sin^2(\alpha^{(1)}_{(+)})-\sin^2(\alpha^{(1)}_{(-)})][\sin^2(\alpha^{(2)}_{(+)})-\sin^2(\alpha^{(2)}_{(-)})]}{[\sin(\alpha^{(1)}_{(+)})\sin(\alpha^{(2)}_{(+)})-\sin(\alpha^{(1)}_{(-)})\sin(\alpha^{(2)}_{(-)})]^2+4\sin(\alpha^{(1)}_{(-)})\sin(\alpha^{(1)}_{(+)})\sin(\alpha^{(2)}_{(-)})\sin(\alpha^{(2)}_{(+)})\sin^2\gamma}\ ,\tag{14}$$

where

$$\gamma=\frac{q(d_1+d_2)(1-\xi)}{2}\quad\text{with}\quad\xi=\frac{2b}{d_1+d_2}\ .\tag{15}$$

Note that although the wave functions (5) depend on our choice of the origin (the breakdown of b into b_1 and b_2), this choice is irrelevant once we have made the assumption of no barrier at the interface; consequently the coefficients R and T depend only on $b\equiv b_1+b_2$ as can be expected on physical grounds (the phase of r still contains a dependence on b_1-b_2).

Figures 2 and 3 illustrate the situation when the "conduction"-band edges of two crystals coincide. Figure 2 corresponds to the case $d_2/d_1=1.5$ and the strengths of the δ potentials ($U_1=-3\pi/2$ and $U_2\approx 0.3U_1$) arranged so that the edges of the lowest bands are at the same energy [see Fig. 2(a)]. The curves 1–3 in Fig. 2(b) show the dependence of $R\equiv 1-T$ on k_1d_1, calculated from Eq. (14) for two different values of the "phase" γ, corresponding to $b=d_1$ (or $b=d_2$, which gives the same result) and $b=(d_1+d_2)/2$. Figure 3 shows similar dependences for the case $d_1/d_2=3$ with the potentials chosen so as to have the bottom of the third band of the left crystal coincide with that of the first band of the right crystal ($U_1=-3\pi/2$ and $U_2\approx 3U_1/2$). Figures 2(c) and 3(c), discussed at the end of Sec. V, describe the reflection coefficient in the vicinity of the band edges; these curves are calculated within the effective-mass approximation corresponding to rigorous matching conditions for the envelope functions, derived in Sec. V.

It can be seen from these figures that in the limit $k_1,k_2\to 0$ the transmission coefficient vanishes, $R\to 1$, unless $\sin\gamma=0$. This can be also shown analytically: Using Eqs. (3) in the limit of small k_1d_1 and k_2d_2, we can bring Eq. (14) into the form

$$T=\frac{4k_1d_1k_2d_2}{\tan(qd_1/2)\tan(qd_2/2)\left[\dfrac{k_1d_1}{\tan(qd_1/2)}+\dfrac{k_2d_2}{\tan(qd_2/2)}\right]^2+U_1U_2\dfrac{\sin(qd_1)\sin(qd_2)}{(qd_1)(qd_2)}\sin^2\gamma}\ .\tag{16}$$

Only in the special case of $\sin^2\gamma=0$, corresponding, e.g., to $\xi=1$ [or $b=(d_1+d_2)/2$], does the transmission coefficient tend to a finite value at small k. The smaller the value of $\sin^2\gamma$ the sharper is the rise of R near $k\to 0$. The strong dependence of T and R on b is noteworthy, because it means that any realistic calculation of the electronic transmission must begin with an accurate evaluation of the atomic positions near the boundary.

The sharp rise of R near $k_1d_1=\pi$, evident from Fig. 3(b) is owing to the fact that the tops of the allowed bands of the two crystals in this example are close but not equal to each other. It can be easily seen from Eq. (14) that $T\to 0$ if $k_1d_1\to\pi$ while $k_2d_2<\pi$.

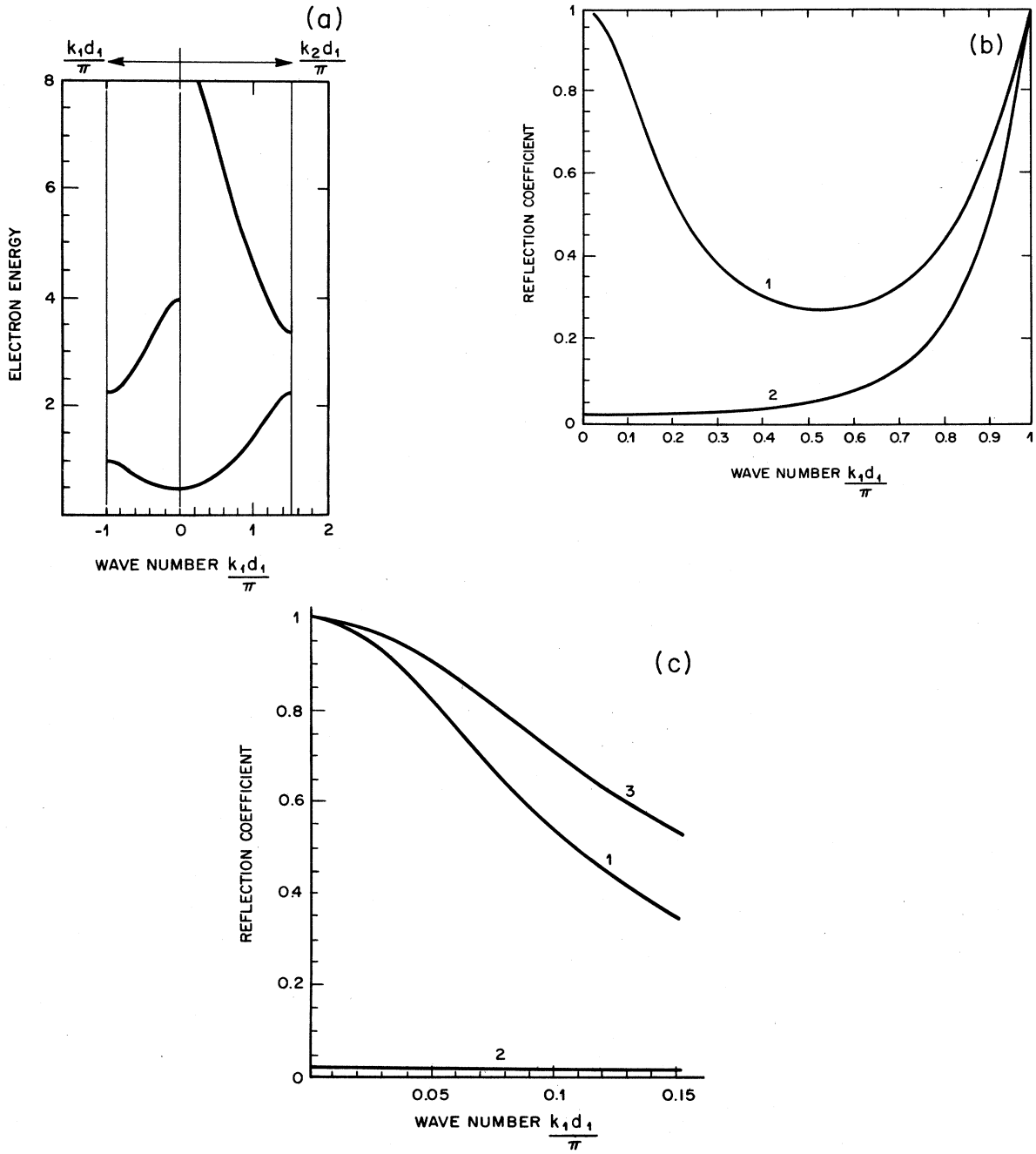

FIG. 2. Electron transmission across the interface of two Kronig-Penney crystals with coincident lowest-band edges. Structure parameters: $d_2/d_1=1.5$, $U_1=-3\pi/2$, and $U_2\approx 0.3U_1$. (a) Dispersion relations in the two crystals; the energy is plotted in units of $\pi^2\hbar^2/2m_0d_1^2$. (b) Reflection coefficient, calculated with the help of Eq. (14) for $b=d_i$ (curve 1) and $b=(d_1+d_2)/2$ (curve 2, corresponds to $\gamma=0$). (c) Reflection coefficient in the vicinity of the band edges, calculated within the effective-mass approximation Eq. (29) with $m_1=1.25m_0$ and $m_2=1.05m_0$ calculated from (24b), and $\zeta_1=0.745$ and $\zeta_2=0.60$ calculated form (28). Curves 1 and 2 are labeled as in (b) and curve 3 corresponds to $b=0.35(d_1+d_2)$.

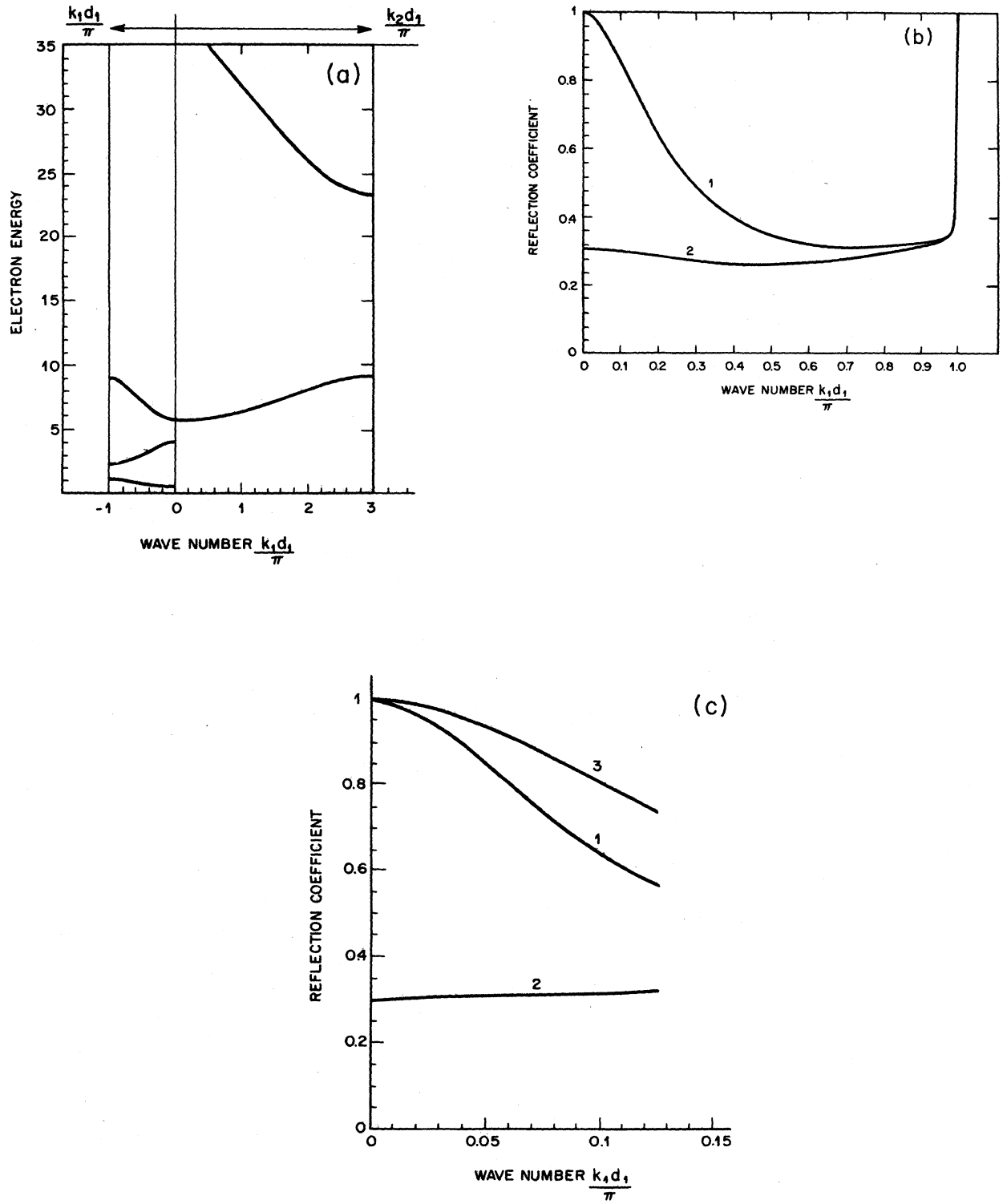

FIG. 3. Electron transmission across the interface of two Kronig-Penney crystals for the case when incident electrons are moving in a higher-lying band and transmitted electrons in the ground band. (a) Dispersion relations plotted as in Fig. 2 in units of $\pi^2\hbar^2/2m_0d_1^2$. The structure parameters, $d_1/d_2=3$, $U_1=-3\pi/2$, and $U_2\approx 3U_1/2$ are chosen so as to have the bottom of the third band of the left crystal coincide with that of the first band of the right crystal. (b) Reflection coefficient, calculated with the help of Eq. (14) for $b=d_i$ (curve 1) and $b=(d_1+d_2)/2$ (curve 2, corresponds to $\gamma=0$). (c) Reflection coefficient in the vicinity of the band edges, calculated within the effective-mass approximation Eq. (29) with $m_1=0.096m_0$ (third band) and $m_2=1.45m_0$ calculated from (24b), and $\zeta_1=0.745$ and $\zeta_2=0.60$ calculated from (28). Curves 1 and 2 are labeled as in (b) and curve 3 corresponds to $b=0.35(d_1+d_2)$.

IV. REFLECTION COEFFICIENT IN THE ENVELOPE-FUNCTION APPROACH

The full Bloch functions Ψ_{k_i} in the constituent crystals are rarely known in practice. It is a common approach, therefore, to replace Ψ of Eq. (7) by an envelope function Φ,

$$\Phi(x)=\begin{cases} e^{ik_1x}+re^{-ik_1x}, & x\le 0 \\ te^{ik_2x}, & x\ge 0 \end{cases} \tag{17}$$

which represents a combination of plane-wave solutions to the effective-mass Hamiltonian,

$$H^{(i)}=E_n^{(i)}-\frac{\hbar^2}{2m_i}\frac{\partial^2}{\partial x^2}, \quad i=1,2 \tag{18}$$

describing electronic motion near the band edges $E_n^{(i)}$ in each crystal. The continuity condition (8) of the full Bloch function Ψ and its derivatives automatically guarantees conservation of the particle flux across the boundary; this condition, however, cannot be applied to Φ and Φ'. In order to avoid contradiction, one can impose the condition of continuity on Φ and $(1/m)(\partial\Phi/\partial x)$, which insures the conservation of flux since the group velocities of electrons in the effective-mass approximation are given by $\hbar k_i/m_i$. This approach leads to a reflection amplitude of the form

$$r=\frac{(k_1/m_1)-(k_2/m_2)}{(k_1/m_1)+(k_2/m_2)} . \tag{19}$$

In particular, if the edges of the two crystal bands coincide, so that $k_1^2/m_1=k_2^2/m_2$, then the reflection amplitude

$$r=-\frac{\sqrt{m_1}-\sqrt{m_2}}{\sqrt{m_1}+\sqrt{m_2}}=-\frac{k_1-k_2}{k_1+k_2}$$

is different by the sign only from (and the reflection coefficient is identical to) the well-known expression for a free electron incident on a step potential barrier. This approach is usually not supported by any justification, except for the absence of relevant information specifying the discontinuity in Φ, which would characterize a given crystal interface. As discussed in the Introduction, a more consistent approach[1] corresponds to letting *both* Φ and Φ' be discontinuous at the interface,

$$\begin{aligned} &\beta_1\Phi(0^-)=\beta_2\Phi(0^+) , \\ &\alpha_1[\partial\Phi(0^-)/\partial x]=\alpha_2[\partial\Phi(0^+)/\partial x] . \end{aligned} \tag{20}$$

Continuity of the flux (in the effective-mass approximation) in this case requires that

$$\alpha_1\beta_1 m_1=\alpha_2\beta_2 m_2 . \tag{21}$$

The reflection amplitude and the transmission coefficient are then given by the following expressions:

$$\begin{aligned} r&=\frac{(k_1/\zeta_1m_1)-(k_2/\zeta_2m_2)}{(k_1/\zeta_1m_1)+(k_2/\zeta_2m_2)} , \\ T&=\frac{4(k_1/\zeta_1m_1)(k_2/\zeta_2m_2)}{[(k_1/\zeta_1m_1)+(k_2/\zeta_2m_2)]^2} \end{aligned} \tag{22}$$

which depend on the ratio $\zeta_1/\zeta_2\equiv\beta_1^2/\beta_2^2$. This ratio represents a (usually unknown) characteristic of the interface. If $\zeta_1/\zeta_2=1$, then Eq. (22) coincides with (19). As will be shown in the next section, for some model interfaces the ζ's can be expressed in terms of the crystal parameters and the band-edge electron energy; in general, however, they have no direct relation to the Bloch functions of constituent crystals.

V. EXACT RESULTS NEAR THE BAND EDGES; THE EFFECTIVE-MASS APPROXIMATION

The effective-mass description of electronic motion in each of the constituent crystals is applicable near the band edges. Consider those edges which correspond in the reduced-zone picture to $k\to 0$. In this limit, the dispersion equation (3) has two types of solution, defining the band edges $E_n\equiv\hbar^2q_n^2/2m_0$ (here we shall suppress the indices $i=1,2$ of the crystals),

$$\tan\left[\frac{q_nd}{2}\right]=-\frac{U}{q_nd} \quad (n=1,3,\ldots) , \tag{23a}$$

$$\sin\left[\frac{q_nd}{2}\right]=0 \quad (n=2,4,\ldots) . \tag{23b}$$

For example, the band edges of the left crystal in Figs. 2 and 3 correspond to $q_1=0.716\pi/d_1$, $q_2=2\pi/d_1$, and $q_3=2.36\pi/d_1$. For the right crystal in Fig. 2, $q_1=0.476\pi/d_2$, and in Fig. 3 $q_1=0.787\pi/d_2$. Similar results can be obtained in a straightforward manner for the band edges as $k\to\pi/d$. Near the $k=0$ band edges the electron energy is approximately given by $E_n+\hbar^2k^2/2m_n$. The odd bands, whose extrema are described by Eq. (23a), possess a positive effective mass m_n for a repulsive δ potential ($U<0$), and a negative m_n for $U>0$. The opposite is true for the even bands described by Eq. (23b), cf. Figs. 2(a) and 3(a). The values of the effective mass for the two types of bands can be readily obtained from the dispersion equation (3), giving

$$\frac{m_n}{m_0}=-\frac{U}{(q_nd)^2}\left[1-\frac{2U}{(q_nd)^2+U^2}\right] \quad (n=1,2,\ldots) , \tag{24a}$$

$$\frac{m_n}{m_0}=\frac{U}{(\pi n)^2} \quad (n=2,4,\ldots) . \tag{24b}$$

For our example in Fig. 2 the numerical values of $(m_n)_i$ in units of m_0 are $(m_1)_1=1.25$, $(m_2)_1=-0.12$, $(m_3)_1=0.096$, and $(m_1)_2=1.05$, $(m_2)_2=-0.036$. For the example of Fig. 3, the left crystal is the same as in

Fig. 2 and the right crystal has $(m_1)_2=1.45$, $(m_2)_2=-0.18$. Validity of Eqs. (24) relies on the following two inequalities:

$$(kd)^2 \ll 1 \quad \text{and} \quad q_n d \frac{\hbar^2 k^2}{4 m_n E_n} \ll 1 \ . \tag{25}$$

Considering the electron transmission at $V=0$ and small k_1 and k_2, we can express the result (16) in terms of the effective masses m_1 and m_2. [Here and below we shall suppress the band index n in the effective mass $m_i \equiv (m_n)_i$, $i=1,2$.] To do this we replace in (16) the energy parameter q by q_n and use the dispersion relation. For the case when the bands of both crystals are of the type, described by (23a), we find

$$T = \frac{4 \dfrac{(k_1 d_1)(q_n d_1)}{U_1} \dfrac{(k_2 d_2)(q_n d_2)}{U_2}}{\left[\dfrac{(k_1 d_1)(q_n d_1)}{U_1} + \dfrac{(k_2 d_2)(q_n d_2)}{U_2} \right]^2 + \sin^2 \gamma} \ . \tag{26}$$

For $\gamma=0$ we can reduce (26) to a form reminiscent of (22):

$$R = \left| \frac{(k_1/\zeta_1 m_1)-(k_2/\zeta_2 m_2)}{(k_1/\zeta_1 m_1)+(k_2/\zeta_2 m_2)} \right|^2 , \tag{27}$$

where

$$\zeta_{1,2} \equiv \left[1 - \frac{2U_{1,2}}{U_{1,2}^2 + (q_n d_{1,2})^2} \right]^{-1} \equiv -\frac{U_{1,2}}{(q_n d_{1,2})^2} \frac{m_0}{m_{1,2}} \ . \tag{28}$$

Thus, the coefficients $\zeta_{1,2}$ acquire a concrete form. We see that for higher-lying bands, where $q_n d_{1,2} \gg |U_{1,2}|$, these parameters tend to unity and the simplest envelope-function approximation (19) becomes applicable.

For $\gamma \neq 0$, using the definition (28), we can express (26) in the following form:

$$T = \frac{4(k_1/\zeta_1 m_1)(k_2/\zeta_2 m_2)}{[(k_1/\zeta_1 m_1)+(k_2/\zeta_2 m_2)]^2 + (q_n^2/m_0^2)\sin^2\gamma} \ . \tag{29}$$

Comparing Eq. (29) with (22) we see that although these equations coincide at $\gamma=0$, in general they are different. This shows that the interface of two one-dimensional crystals can be such that the Harrison matching conditions (20) are inadequate. For our numerical examples in Figs. 2 and 3, the reflection coefficients $R=1-T$ calculated with the help of Eq. (29) are plotted in Figs. 2(c) and 3(c), respectively. Numerical values of the coefficients m and ζ, calculated from Eqs. (24a) and (28) and used in the evaluation of (29), are indicated in the captions to these figures.

In the envelope-function approximation, the result (29) can be modeled by considering the transmission of a particle from a medium governed by the Hamiltonian $H^{(1)}$ to that governed by $H^{(2)}$ [Eq. (18)] *through a "vacuum" gap* of thickness $\tilde{b}$, where the particle is assumed to have the free-electron mass m_0, see Fig. 4. Assume that the "band edges" coincide and have a vanishing affinity, $E_n^{(1)}=E_n^{(2)}=0$, so that there are no potential steps at the vacuum interfaces. Application of Harrison's matching conditions (20) and the continuity conditions (21) at each interface (taking, without a loss of generality, for the vacuum $\alpha_0=\beta_0=1$) then leads to an expression of the form (29), with $\gamma \equiv q\tilde{b}$, $q \equiv (2m_0 E/\hbar)^2$, and $\zeta_i \equiv \beta_i^2$. Thus we conclude that in the general one-dimensional case the envelope-function matching can be accomplished with *three* parameters: α, β, and γ (equivalently, in the effective-mass approximation with m, ζ, and γ).

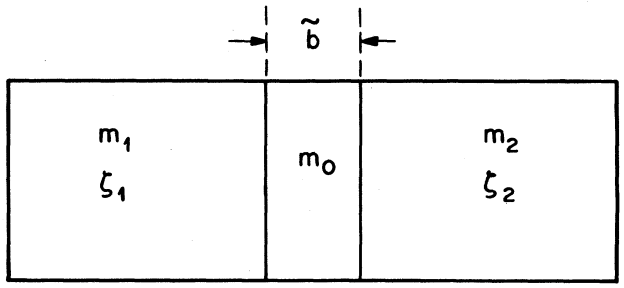

FIG. 4. Illustration of an envelope-function model which results in the same transmission coefficient as that given by Eq. (29) if Harrison's matching conditions (20) and (21) are used at each interface.

VI. FURTHER EXAMPLES; IMPEDANCE MATCHING

In the numerical examples given so far we have considered the case where the band edges of two crystals were degenerate at the interface. Let us now look at the more general situation. A misalignment of band edges can be produced by varying the crystal parameters (U and/or d) or by introducing a potential step at the $x=0$ plane defining the interface. Such a potential step can be thought of as produced by an interfacial layer[24] of infinitesimal extent.

Consider this situation first. Figure 5 shows the wave-vector dependence of the electron reflection coefficient for two identical crystals ($U_1=U_2=-3\pi/2$, $d_1=d_2=d$) with a potential step V at the interface $V=\xi(\pi^2\hbar^2/2m_0 d^2)$ and $\xi=0.05$ [Fig. 5(a)] or $\xi=0.1$ [Fig. 5(b)]. Curves 1–3 in Figs. 5(a) and 5(b) were calculated using a general expression for R following from Eq. (11). An interesting feature seen in Figs. 5 is the existence of perfect transmission ($R=0$) at a certain "resonant" energy but only for "ideal" interfaces corresponding to $\gamma=0$. Note that the reflection coefficient calculated in the envelope-function approach,

$$R = \left| \frac{k_1 - k_2}{k_1 + k_2} \right|^2$$

[curves 4 in Figs. 5(a) and 5(b) exhibits no perfect transmission at any energy.

Next, we consider the situation when the misalignment of band edges occurs entirely due to different band struc-

tures of constituent crystals without a potential step at the interface. In this case, illustrated in Figs. 6 and 7, calculation of the reflection coefficient can be done, directly from Eq. (14) for the examples of Figs. 2 and 3. Figure 6 describes a case, similar to that presented in Fig. 2 ($d_2/d_1=1.5$ and $U_1=-3\pi/2$), except that now $U_2=0.5U_1$, producing a higher lowest-band edge in crystal 2 as shown in Fig. 6(a). This example describes the transmission between the ground bands of both crystals. Again, for $\gamma=0$ we observe perfect transmission at a certain energy. The possibility that quantum reflections at an abrupt heterojunction interface may vanish for some energy has been discussed by Levi and Chiu[25] in connection with the fundamental limits of hot-electron transistors; by analogy with microwave transmission lines this situation was termed[25] "impedance matching." In the simplest plane-wave effective-mass approximation de-

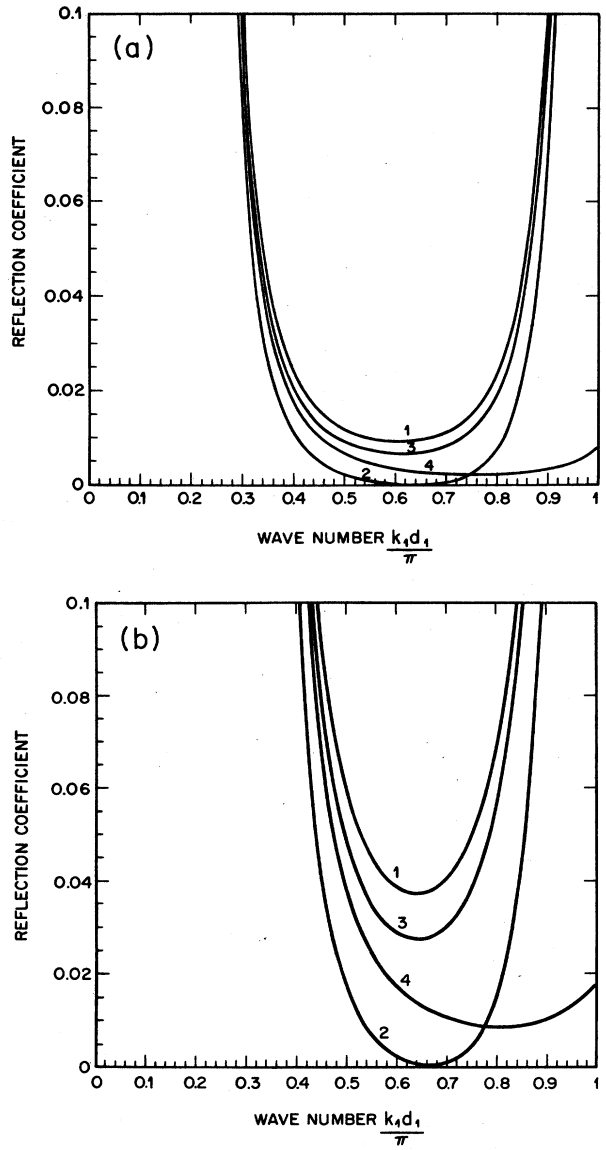

FIG. 5. Reflection coefficient for two identical crystals ($U_1=U_2=-3\pi/2$, $d_1=d_2=d$) with a potential step V at the interface $V\equiv\xi(\pi^2\hbar^2/2m_0d^2)$ [(a) $\xi=0.05$ and (b) $\xi=0.1$]. Curves 1–3 are calculated with the help of Eq. (11) and curves 4 within the envelope-function approach using exact dispersion relations.

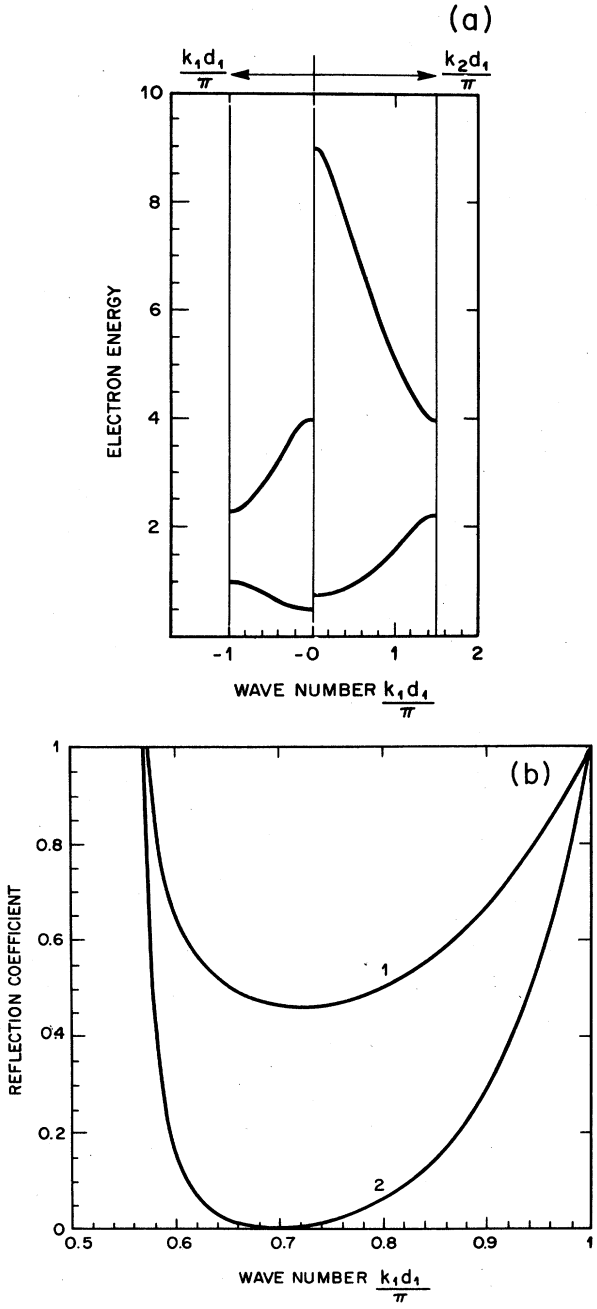

FIG. 6. Electron transmission for the case when incident and transmitted electrons are moving in the ground band of the respective crystals, but the band edges are not aligned at the interface. (a) Dispersion relations in the two crystals plotted as in Fig. 2 in units of $\pi^2\hbar^2/2m_0d_1^2$. The structure parameters are similar to those in Fig. 2 except for $U_2=0.5U_1$. The effective mass in the lowest band of the right crystal in this example equals $1.09m_0$. (b) Reflection coefficient, calculated with the help of Eq. (14) for $b=d_i$ (curve 1) and $b=(d_1+d_2)/2$ (curve 2, corresponds to $\gamma=0$).

scribed by Eq. (19), the impedance-matched condition arises when the electron velocities k_i/m_i are the same on either side of the junction.

Figure 7 illustrates the situation similar to that considered in connection with Fig. 3, when the transmission occurs from a higher-lying band of crystal 1 to the ground band of crystal 2. The structure parameters ($d_1/d_2=3$, $U_1=-3\pi/2$, and $U_2=1.8U_1/2$) are again chosen so as to produce an upward step in the corresponding band edges, as shown in Fig. 7(a). As seen from Fig. 7(b), no perfect impedance matching happens in this example for any value of γ. That this was going to be the case could be surmised already from the band-structure

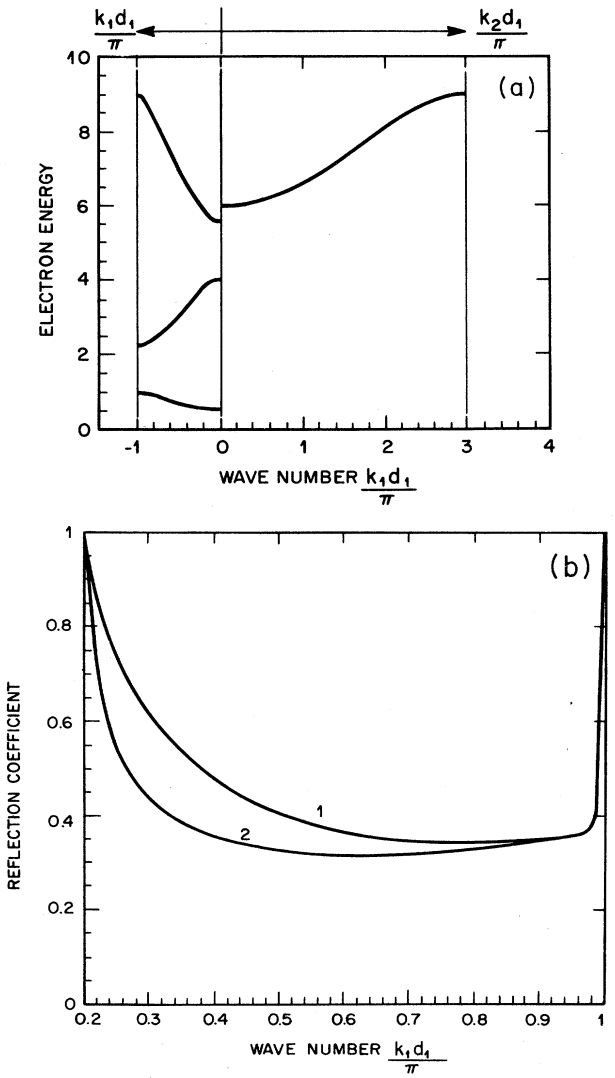

FIG. 7. Electron transmission across the interface of two Kronig-Penney crystals for the case when incident electrons are moving in a higher-lying band and transmitted electrons in the ground band. (a) Dispersion relations in the two crystals, plotted in units of $\pi^2\hbar^2/2m_0d_1^2$. The structure parameters are similar to those in Fig. 2 except for $U_2=1.8U_1$. The effective mass in the lowest band of the right crystal is $1.96m_0$. (b) Reflection coefficient, calculated with the help of Eq. (14) for $b=d_i$ (curve 1) and $b=(d_1+d_2)/2$ (curve 2, corresponds to $\gamma=0$).

diagram in Fig. 7(a): At all coincident energy levels in the allowed bands of the two crystals, the electron group velocity is manifestly higher in the left crystal.

VII. CONCLUSION

Using the simplest soluble Kronig-Penney model of two one-dimensional crystals, we have obtained an exact solution for the problem of electron transmission across the interface of such crystals. This solution allowed us to compare and assess the widely used envelope-function (plane-wave) approximations of different degrees of refinement. It turns out that *neither* the simplest such approximation, corresponding to a continuous envelope function Φ and a discontinuous gradient Φ' (with a single-parameter matching of the electron flux $m^{-1}\Phi'$ across the interface) *nor* the refined procedure, proposed by Harrison[1] [corresponding to a two-parameter matching of discontinuous Φ and Φ', cf. Eq. (20), subject to the flux-continuity condition], produce in general an adequate description. Even near the band edges where the effective-mass approximation in the constituent crystals is excellent, a rigorous plane-wave approximation requires *three* parameters: Harrion's α and β and another coefficient γ describing the size of the crystal cell at the interface. The geometric meaning of γ within our model is discussed at the end of the Sec. V; for a more general one-dimensional model γ can be expected to provide a reasonable phenomenological parameterization of the transmission problem. Only for a special type of boundary, corresponding in our model to $\gamma=0$, does Harrison's description provide a reasonable approximation. In this case, we were able to derive an exact expression for his coefficients α and β near the band edges. This expression gives the dependence of these coefficients on the band-edge energy and shows that for the higher-lying bands even the simpler one-parameter effective-mass matching of Φ' becomes adequate.

In practice, the question of electron transmission across the interface of distinct crystals arises mainly in the analysis of heterostructure transport problems. To the extent that our essentially one-dimensional analysis can shed any light on these problems, we can expect that lattice-matched heterostructures do correspond to a special type of the boundary with $\gamma=0$ and consequently Harrison's approach is relevant. However, as has been appreciated by a number of authors,[4,10,17] in three dimensions it is impossible to match the Bloch solutions of two different crystals across a continuous boundary surface, which corresponds to the fact that for a given energy in the allowed band, Bloch solutions do not form a complete set in the double crystal. In that case, inclusion of the evanescent states, exponentially localized near the interface and degenerate with the allowed-band Bloch states, is mandatory. As briefly discussed at the end of Sec. II, the evanescent states do *not* come into play in the transmission problem for band electrons in the one-dimensional case considered here. The reason we are able to get away without taking these states into account is due to the fact that in one dimension the evanescent-state energies are strictly within the forbidden gaps and

so they do not mix with the Bloch states, in contrast to a three-dimensional (or two-dimensional) situation. Perhaps the effect of the evanescent states in three dimensions could be modeled phenomenologically with a vacuum gap parameter γ, as in Fig. 4. It is an interesting and largely open question, whether one could obtain a reasonable description of the general three-dimensional interface transmission problem in an envelope-function approach with three phenomenological parameters, α, β, and γ.

Note added in proof. After submitting this manuscript for publicaton, we became aware of two papers by Witold Trzeciakowski: Phys. Rev. B **38**, 4322 (1988); **38**, 12 493 (1988), where questions of the effective-mass approximation and the boundary conditions in heterostructures are discussed on the basis of a one-dimensional analysis, in some respects similar to ours. While we share many of Trzeciakowski's conclusions, most of our results do not overlap.

ACKNOWLEDGMENT

We are grateful to M. D. Stiles for a helpful discussion.

[1]W. A. Harrison, Phys. Rev. **123**, 85 (1961).
[2]E. Caruthers and P. J. Lin-Chung, Phys. Rev. B **17**, 2705 (1978).
[3]G. A. Sai-Halasz, L. Esaki, and W. Harrison, Phys. Rev. B **18**, 2812 (1978).
[4]G. C. Osbourn and D. L. Smith, Phys. Rev. B **19**, 2124 (1979).
[5]J. N. Schulman and T. C. McGill, Phys. Rev. B **19**, 6341 (1979).
[6]J. Ihm, P. K. Lam, and M. L. Cohen, Phys. Rev. B **20**, 4120 (1979).
[7]W. Andreoni and R. Car, Phys. Rev. B **21**, 3334 (1980).
[8]Y.-C. Chang and J. N. Schulman, J. Vac. Sci. Technol. **21**, 540 (1982).
[9]A. C. Marsh and J. C. Inkson, J. Phys C **17**, 6561 (1984).
[10]M. D. Stiles and D. R. Hamann, Phys. Rev. B **38**, 2021 (1988).
[11]D. J. BenDaniel and C. B. Duke, Phys. Rev. **152**, 683 (1966).
[12]R. A. Morrow and K. R. Brownstein, Phys. Rev. B **30**, 678 (1984).
[13]H. C. Liu, Superlatt. Microstruct. **3**, 413 (1987).
[14]W. Pötz and D. K. Ferry, Superlatt. Microstruct. **3**, 57 (1987).
[15]P. J. Price, in *Proceedings of the International Conference on the Physics of Semiconductors, Exeter, 1962* (Institute of Physics and the Physical Society, London, 1962), pp. 99–103.
[16]G. Bastard, Phys. Rev. B **24**, 5693 (1981).
[17]S. R. White and L. J. Sham, Phys. Rev. Lett. **47**, 879 (1981); S. R. White, G. E. Margues, and L. J. Sham, J. Vac. Sci, Technol. **21**, 544 (1982).
[18]H. Kroemer and Q.-G. Zhu, J. Vac. Sci. Technol. **21**, 551 (1982); Q.-G. Zhu and H. Kroemer, Phys. Rev. B **27**, 3519 (1983).
[19]M. Altarelli, Phys. Rev. B **28**, 842 (1983).
[20]A. Sasaki, Phys. Rev. B **30**, 7016 (1984); Surf. Sci. **174**, 624 (1986).
[21]M. Babiker and B. K. Ridley, Superlatt. Microstruct. **2**, 287 (1986).
[22]R. de L. Kronig and W. G. Penney, Proc. R. Soc. London, Ser. A **130**, 499 (1931).
[23]These states are similar to the well-known Tamm states, localized near crystal surfaces [I.E. Tamm, Z. Phys. **76**, 849 (1932)]. A simple calculation of surface states for one-dimensional crystal models has been presented by M. Tomásek, Czech. J. Phys. B **12**, 159 (1962).
[24]F. Capasso, A. Y. Cho, K. Mohammed, and P. W. Foy, Appl. Phys. Lett. **46**, 664 (1985).
[25]A. F. J. Levi and T. H. Chiu, Appl. Phys. Lett. **51**, 984 (1987).